EPJ Web of Conferences **353**, 01012 (2026) https://doi.org/10.1051/epjconf/202635301012
mm Universe 2025

CHEX-MATE: Joint fit of the universal pressure profile and galaxy cluster masses

M. Muñoz-Echeverría[1*], E. Pointecouteau[1], G. W. Pratt[2], J.-F. Macías-Pérez[3], M. Douspis[4], L. Salvati[4], I. Bartalucci[5], H. Bourdin[6,7], N. Clerc[1], F. De Luca[6,7], M. De Petris[8], M. Donahue[9], S. Dupourqué[1], D. Eckert[10], S. Ettori[11,12], M. Gaspari[13], F. Gastaldello[5], M. Gitti[14,15], A. Gorce[4], S. Ilić[16], S. T. Kay[17], J. Kim[18], L. Lovisari[5,19], B. J. Maughan[20], P. Mazzotta[6,7], L. McBride[4], J.-B. Melin[21], F. Oppizzi[22]E. Rasia[23,24,25], M. Rossetti[5], H. Saxena[26], J. Sayers[26], M. Sereno[11,12], M. Tristram[16]

[1]IRAP, CNRS, Université de Toulouse, CNES, UT3-UPS, (Toulouse), France
[2]Université Paris-Saclay, Université Paris Cité, CEA, CNRS, AIM, 91191, Gif-sur-Yvette, France
[3]Université Grenoble Alpes, CNRS, LPSC-IN2P3, 53, avenue des Martyrs, 38000 Grenoble, France
[4]Université Paris-Saclay, CNRS, Institut d'Astrophysique Spatiale, 91405, Orsay, France
[5]INAF, Istituto di Astrofisica Spaziale e Fisica Cosmica di Milano, via A. Corti 12, 20133 Milano, Italy
[6]Dipartimento di Fisica, Università degli studi di Roma Tor Vergata, Via della Ricerca Scientifica 1, I-00133 Roma, Italy
[7]INFN, Sezione di Roma 'Tor Vergata', Via della Ricerca Scientifica, 1, 00133, Roma, Italy
[8]Dipartimento di Fisica, Sapienza Università di Roma, Piazzale Aldo Moro 5, I-00185 Rome, Italy
[9]Michigan State University (MSU) - Dept of Physics and Astronomy, 567 Wilson Road, East Lansing, Michigan, 48824, USA
[10]Department of Astronomy, University of Geneva, Ch. d'Ecogia 16, CH-1290 Versoix, Switzerland
[11]INAF - Osservatorio di Astrofisica e Scienza dello Spazio di Bologna, via Piero Gobetti 93/3, I-40129 Bologna, Italy
[12]INFN, Sezione di Bologna, viale Berti Pichat 6/2, I-40127 Bologna, Italy
[13]Department of Physics, Informatics and Mathematics, University of Modena and Reggio Emilia, 41125 Modena, Italy
[14]Dipartimento di Fisica e Astronomia (DIFA), Alma Mater Studiorum - Università di Bologna, via Gobetti 93/2, 40129 Bologna, Italy
[15]Istituto Nazionale di Astrofisica – Istituto di Radioastronomia (IRA), via Gobetti 101, 40129 Bologna, Italy
[16]IJCLab, Université Paris-Saclay, CNRS/IN2P3, IJCLab, 91405 Orsay, France
[17]Jodrell Bank Centre for Astrophysics, Department of Physics and Astronomy, The University of Manchester, Manchester M13 9PL, UK
[18]Department of Physics, Korea Advanced Institute of Science and Technology (KAIST), 291 Daehak-ro, Yuseong-gu, Daejeon 34141, Republic of Korea
[19]Center for Astrophysics | Harvard & Smithsonian, 60 Garden Street, Cambridge, MA 02138, USA
[20]HH Wills Physics Laboratory, University of Bristol, Bristol, UK
[21]IRFU, CEA, Université Paris-Saclay, 91191, Gif-sur-Yvette, France
[22]INFN-Sezione di Genova, Via Dodecaneso 33, 16146, Genova, Italy
[23]INAF, Osservatorio Astronomico di Trieste, via Tiepolo 11, I-34131, Trieste, Italy
[24]IFPU, Institute for Fundamental Physics of the Universe, Via Beirut 2, 34014 Trieste, Italy
[25]Department of Physics; University of Michigan, Ann Arbor, MI 48109, USA
[26]California Institute of Technology, 1200 East California Boulevard, Pasadena, California, USA

*miren.munoz-echeverria@irap.omp.eu

© The Authors, published by EDP Sciences. This is an open access article distributed under the terms of the Creative Commons Attribution License 4.0 (https://creativecommons.org/licenses/by/4.0/).

Abstract. Within the self-similar framework of structure formation, the thermal pressure of the hot intra-cluster medium follows a universal distribution that is independent of the cluster mass scale. Once normalised to the proper mass and redshift dependencies, this pressure distribution becomes common to all clusters. Reconstructing such a universal pressure profile requires individual estimates of each cluster's mass. In this work, we present a methodology to simultaneously fit the universal pressure profile alongside the masses of individual clusters in a sample, while properly accounting for correlations between the profile's shape, its amplitude, and cluster masses. We apply this method to a sub-sample of clusters from the CHEX-MATE project and demonstrate the strong impact that the assumed pressure profile has on the measured signal. This effect propagates into the thermal Sunyaev-Zel'dovich (tSZ) power spectrum and, in turn, influences the determination of cosmological parameters.

1 Introduction

Galaxy clusters are formed through the accretion of matter driven by gravity, and as a result, they are scaled versions of one another [1, 2]. Consequently, the distribution of thermal pressure within clusters becomes universal once it is normalised with respect to mass and redshift [3, 4]. The so-called universal pressure profile (UPP) is a fundamental ingredient for both cluster detection techniques and cosmological studies based on millimetre-wave observations (e.g., [5, 6]). However, as mentioned above, its reconstruction requires scaling the pressure profiles of individual clusters according to their masses. Ideally, the true cluster masses would be used for this purpose, but direct measurements are not feasible from observations, meaning that reliable mass estimates are necessary [7].

In this work, we propose a method that allows for the simultaneous fitting of the UPP and the masses of individual clusters. We present this approach in the context of the "Cluster HEritage project with *XMM-Newton* - Mass Assembly and Thermodynamics at the Endpoint of structure formation" (CHEX-MATE[1], [8]). This is a multi-year *XMM-Newton* Heritage programme designed to investigate the interplay between gravitational and non-gravitational processes in clusters, and their impact on cluster mass estimations. The complete CHEX-MATE sample comprises 118 thermal Sunyaev-Zel'dovich (tSZ) selected *Planck* clusters. In this paper, we concentrate on the "Data Release 1" (DR1) sub-sample described in [9].

The CHEX-MATE project provides multi-wavelength coverage, spanning X-ray, radio, millimetre, optical, and infrared observations [8]. For the present analysis, we make use of X-ray and millimetre data to derive thermal pressure profiles. Fig. 1 shows the individual profiles reconstructed separately from *XMM-Newton* observations (in orange, extracted with the CHEX-MATE pipeline) and from *Planck* data (in blue, obtained following the method in [11]) for each cluster. By combining both data sets we achieve broad radial coverage of the pressure distributions. Furthermore, our fits are informed by 'dynamical mass' estimates derived from the velocity dispersions of cluster member galaxies [12]. Hence, our final sample consists of the 24 DR1 clusters for which such dynamical masses were obtained in [12].

2 Model

We assume that the thermal pressure profile of every cluster is well described by:

$$P(r) = P_{500} \times \mathbb{P}(x), \quad \text{with the normalised radius} \quad x \equiv r/R_{500}. \tag{1}$$

[1] http://xmm-heritage.oas.inaf.it/

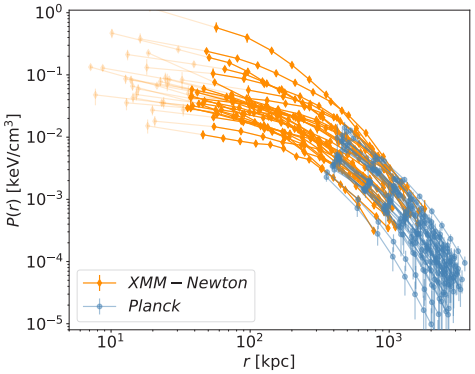

Figure 1. Individual pressure profiles for the 28 DR1 clusters (i.e., the 28 DR1 clusters without *XMM-Newton* off-set pointings). In orange and blue, profiles reconstructed from *XMM-Newton* and *Planck* data, respectively. We refer the reader to [10] for details on the choice of radial binning.

Here r is the physical radius, and R_{500}[2] and P_{500} are functions of the characteristic M_{500}[2] mass and the redshift of each cluster. Following the self-similar model (see Eq. A.1 in [4]), the normalisation factor P_{500} can be defined as:

$$P_{500}(M_{500}, z) = \frac{3}{8\pi}\left[\frac{500G^{-1/4}}{2}\right]^{4/3}\frac{\mu}{\mu_e}f_B\left[M_{\rm pivot}\right]^{2/3} \times\ H(z)^{8/3}\left[\frac{M_{500}}{M_{\rm pivot}}\right]^{\delta}. \tag{2}$$

The parameter δ describes the evolution of the pressure normalisation with M_{500}, and it can be fitted as a free parameter of the model. Since its value may vary with the dynamical state of the intracluster medium and the nuclear activity of the brightest cluster galaxy [13], the use of a representative cluster sample [8] is essential. In Eq. 2, G is the Newtonian constant of gravitation, $H(z)$ is the Hubble parameter, f_B denotes the cosmic baryon fraction, and μ and μ_e are respectively the mean molecular weight and the mean molecular weight per free electron. We consider $M_{\rm pivot} = 3 \times 10^{14}$ M$_\odot$ to be consistent with [4].

In Eq. 1, the second term corresponds to the universal pressure profile that we aim at fitting. Following previous works in the literature [3, 4, 11, 14–18], we model the UPP as a generalised Navarro-Frenk-White (gNFW, [3]) profile:

$$\mathbb{P}(x) = \frac{P_0}{(c_{500}x)^\gamma\,[1 + (c_{500}x)^\alpha]^{(\beta-\gamma)/\alpha}}. \tag{3}$$

And finally, we account for possible systematic discrepancies between X-ray and tSZ-derived (*XMM-Newton* and *Planck*, in our case) pressure profiles by fitting also η_T:

$$\eta_T \sim P^{\rm X}/P^{\rm tSZ}. \tag{4}$$

In practice, our model considers that each individual pressure profile $P_{{\rm data},i}$ (Fig. 1) is well described by a multivariate Gaussian distribution

$$\mathcal{L}_i = \frac{1}{\sqrt{(2\pi)^{n_i}|C_i|}}\exp\left[-\frac{1}{2}(P_{{\rm data},i} - P_{{\rm model},i})^T C_i^{-1}(P_{{\rm data},i} - P_{{\rm model},i})\right], \tag{5}$$

with $P_{{\rm model},i}$ the model for cluster i defined in Eq. 1, n_i the number of data pressure bins, and C_i the covariance matrix that accounts for the errors in data pressure profiles ($\Sigma_{{\rm data},i}$) and the intrinsic scatter ($\Sigma_{{\rm int},i}$):

$$C_i(\theta) = \Sigma_{{\rm data},i} + \Sigma_{{\rm int},i}(\theta). \tag{6}$$

We assume a log-normal intrinsic scatter profile and choose to parametrise it as a function of the scaled radius x, following:

$$\sigma_{\rm int}(x) = \sigma_1 \exp\left[-\omega x\right] + \sigma_0 x, \tag{7}$$

[2] M_{500} and R_{500} are defined as $M_{500} = (4/3)\pi R_{500}^3 \times 500\rho_{\rm crit}$ where $\rho_{\rm crit}(z) = 3H(z)^2/(8\pi G)$ is the critical density of the Universe at the cluster redshift z.

with σ_1, σ_0, and ω the free parameters in the model. Thus, each diagonal element of $\Sigma_{\mathrm{int},i}$ is defined as:

$$\begin{aligned}\Sigma^{k,k}_{\mathrm{int},i}(\theta) &= \left[P_{\mathrm{model},i}(r_{i,k},\theta) \times \sigma_{\mathrm{int}}(r_{i,k},\theta)\right]^2 \\ &= \left[P_{500,i}(\theta)\ \mathbb{P}(r_{i,k},\theta) \times \sigma_{\mathrm{int}}(r_{i,k},\theta)\right]^2 . \end{aligned} \tag{8}$$

Since pressure profiles are generally expected to vary smoothly, neighbouring points correlating with each other, we introduce a correlation structure into the intrinsic scatter covariance matrix by employing a "radial basis function", also known as a "squared-exponential" kernel. The characteristic scale of the kernel is determined by the parameter L_{int}, and the off-diagonal elements of the intrinsic scatter covariance matrix are expressed as:

$$\Sigma^{k,l}_{\mathrm{int},i}(\theta) = \sqrt{\Sigma^{k,k}_{\mathrm{int},i}\Sigma^{l,l}_{\mathrm{int},i}}\exp\left[-\frac{(x_{i,k}-x_{i,l})^2}{2L^2_{\mathrm{int}}}\right], \tag{9}$$

with $x_{i,k} = r_{i,k}/R_{500,i}$ and $x_{i,l} = r_{i,l}/R_{500,i}$. In summary, our model contains two types of free parameters, θ:

- Global parameters, that is, common to all clusters. These are: the slope in the $P_{500} - M_{500}$ scaling relation (δ); the gNFW parameters of the UPP ($P_0, c_{500}, \alpha, \beta, \gamma$); the parameters characterising the intrinsic scatter ($\sigma_1, \sigma_0, \omega$, and L_{int}); and the ratio between X-ray and tSZ pressure profiles (η_T).
- Individual parameters: one mass parameter per galaxy cluster, $\{M_{500,1}, ..., M_{500,n}\}$. In a fixed cosmology, and assuming a redshift per cluster, the conversion between M_{500} and R_{500} (needed to calculate the x in the model) is straightforward[2].

In this framework, any of the mentioned parameters can be fitted or fixed to a value.

3 Joint UPP and M_{500} measurement

To jointly constrain both the universal pressure profile and the individual cluster masses, we incorporate external information into the fit by adopting Gaussian priors on the masses. Dynamical mass estimates are particularly well suited: although they are subject to scatter, they are considered to be nearly unbiased [19, 20]. According to validation tests performed on simulated data, this property is essential for an unbiased reconstruction of both the UPP and the cluster masses when using our joint-fitting method. Moreover, dynamical mass estimates are largely uncorrelated with the *XMM-Newton* and *Planck* pressure profiles.

We adopt flat priors for all global parameters (with the exception of δ) and Gaussian priors, centred on the dynamical estimates, for the individual mass parameters, and perform a simultaneous fit of the 24 pressure profiles. Given the large number of free parameters involved, an efficient inference method is required. For this reason, we rely on `jax`-based codes [21] that enable a fast Markov chain Monte Carlo sampling. Bayesian inference is carried out using the NUTS sampler [22], as implemented in the `numpyro` library [23].

We show in Fig. 2 the best-fitting individual cluster masses with respect to the dynamical mass estimates. We present three cases: in green, the result obtained by assuming a self-similar evolution of the pressure normalisation with M_{500}, that is, $\delta = 2/3$; in red, considering the $\delta = 2/3 + 0.12$ value from [4]; and, in blue, the masses obtained by letting δ free in the fit, with a Gaussian prior $\mathcal{N}(2/3, 0.2^2)$. By construction, the fitted masses are anchored to the dynamical mass scale through the priors, but they are refined by the pressure distribution.

By jointly fitting the universal pressure profile and cluster masses, we propagate the uncertainties on the individual masses to the UPP. In addition, we are able to refine the dynamical estimates and find the masses that scale the pressure profiles the best: same accuracy, but

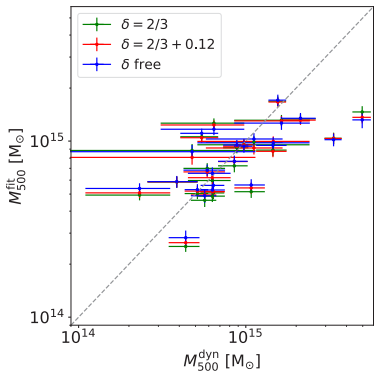

Figure 2. Best-fitting individual cluster masses obtained from the joint fit to data with respect to the dynamical mass estimates used to inform the fit. Green, red, and blue correspond to the fits performed assuming respectively $\delta = 2/3$, $\delta = 2/3 + 0.12$, and δ as a free parameter. Uncertainties of fitted masses are calculated as the standard deviation of the marginalised posterior distribution for each cluster mass parameter.

better precision for M_{500}. Consequently, we also recover the intrinsic scatter in the pressure profiles (Eq. 7), which arises mainly from baryonic physics and differences in the dynamical states of clusters in the sample, without being biased by the scatter present in the mass estimates used for scaling.

Regarding the ratio between X-ray and tSZ data, we find in all three cases a best-fit value of $\eta_T \sim 1.05$. This is consistent with what would be expected from neglecting tSZ relativistic corrections [24].

4 Impact of the UPP on the M_{500} determination

In this section, we examine the intricate relationship between the UPP and cluster mass estimates by exploring how the assumed shape of the UPP influences the derived masses for a given sample. To do this, we fix the parameters of the gNFW profile and the value of δ to those reported in several previous studies (N07 [3], A10 [4], P13 [11], B17 [14], G19 [15], PACT [16], MP23 [17], S23 [18]) and fit the 24 cluster masses to the pressure profiles in Fig. 1. As in the previous section, we adopt Gaussian priors centred on the dynamical mass estimates [12] for all clusters.

In Fig. 3, we present the distributions of the best-fit M_{500} masses obtained under the assumption of each different UPP, allowing η_T to vary for all fits. Circles indicate the average cluster mass across the sample, while diamonds represent the mean mass when fixing $\eta_T = 1.05$ in the fits. These results are compared to the masses obtained from the joint-fitting procedure in the previous section. The figure clearly shows that the assumed gNFW profile shape, together with the adopted mass dependence (via δ), have a strong impact on the measured signal. The mean cluster mass scales obtained by fixing different UPPs differ by 10 to 50%. This highlights the necessity for a coherent treatment of both the UPP and the cluster mass scale to avoid bias in cosmological analyses such as [6].

In addition, when adopting the UPP parameters from A10 [4], we fall back on masses that are compatible with those derived from *Planck* data using the MMF3 algorithm [5]. Since MMF3 extracts the signal under the assumption of the A10 profile, this serves as an important consistency check, demonstrating the robustness of our methodology.

5 Summary and conclusions

In summary, we have presented here a framework to jointly fit the universal pressure profile and individual cluster masses. To provide prior information on the mass scale, we employed dynamical mass estimates, which, although scattered, are essentially unbiased and uncorrelated with the fitted pressure profiles.

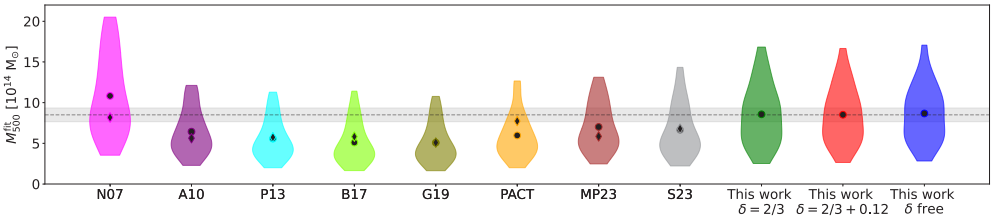

Figure 3. Best-fit M_{500} mass distributions obtained by assuming different UPPs from the literature, compared to the masses from the joint UPP and mass fit in Sect. 3. See text for details. As a reference, the horizontal grey area indicates $8.50 \pm 0.85 \times 10^{14}$ $M_\odot$.

By adopting this joint-fitting strategy, we improve on the determination of individual M_{500} values, making direct use of the thermal pressure distribution. In addition, the uncertainties on the masses are naturally propagated to the UPP, and therefore, could be subsequently propagated to the tSZ cosmological analyses.

We have also quantified the influence of the assumed UPP shape on the cluster mass estimates derived from thermal pressure profiles. Our results confirm a strong correlation between the adopted pressure profile and the corresponding mass scale, and therefore, the need for a self-consistent framework.

References

[1] Rosati, P., Borgani, S., & Norman, C. 2002, ARA&A, 40, 539
[2] Voit, G. M. 2005, Reviews of Modern Physics, 77, 207
[3] Nagai, D., Kravtsov, A. V., & Vikhlinin, A. 2007, ApJ, 668, 1
[4] Arnaud, M., Pratt, G. W., Piffaretti, R., *et al.* 2010, A&A, 517, A92
[5] Melin, J. B., Bartlett, J. G., & Delabrouille, J. 2006, A&A, 459, 341
[6] Salvati, L., Douspis, M., & Aghanim, N. 2018, A&A, 614, A13
[7] Pratt, G. W., Arnaud, M., Biviano, A., *et al.* 2019, Space Sci. Rev., 215, 25
[8] CHEX-MATE Collaboration, Arnaud, M., Ettori, S., *et al.* 2021, A&A, 650, A104
[9] Rossetti, M., Eckert, D., Gastaldello, F., *et al.* 2024, A&A, 686, A68
[10] Muñoz-Echeverría, M., Pointecouteau, E., Pratt, G. W., *et al.* 2025, A&A, 704, A302
[11] Planck Collaboration, Ade, P. A. R., Aghanim, N., *et al.* 2013, A&A, 550, A131
[12] Sereno, M., Maurogordato, S., Cappi, A., *et al.* 2025, A&A, 693, A2
[13] Battaglia, N., Bond, J. R., Pfrommer, C., *et al.* 2012, ApJ, 758, 2, 75
[14] Bourdin, H., Mazzotta, P., Kozmanyan, A., *et al.* 2017, ApJ, 843, 72
[15] Ghirardini, V., Eckert, D., Ettori, S., *et al.* 2019, A&A, 621, A41
[16] Pointecouteau, E., Santiago-Bautista, I., Douspis, M., *et al.* 2021, A&A, 651, A73
[17] Melin, J. B. & Pratt, G. W. 2023, A&A, 678, A197
[18] Sayers, J., Mantz, A. B., Rasia, E., *et al.* 2023, ApJ, 944, 221
[19] Gavazzi, R. 2005, A&A, 443, 793
[20] Ferragamo, A., Barrena, R., Rubiño-Martín, J. A., *et al.* 2021, A&A, 655, A115
[21] Bradbury, J., Frostig, R., Hawkins, P., *et al.* 2018, JAX: composable transformations of Python+NumPy programs
[22] Hoffman, M. D. & Gelman, A. 2014, Journal of Machine Learning Research, 15, 1593
[23] Phan, D., Pradhan, N., & Jankowiak, M. 2019, arXiv e-prints, arXiv:1912.11554
[24] Perrott, Y. 2024, PASA, 41, e087